Neuroscience Letters 468 (2010) 353–358

Contents lists available at ScienceDirect

Neuroscience Letters

journal homepage: www.elsevier.com/locate/neulet

Distinct brain networks for time-varied characteristics of acupuncture

Jixin Liu[a,b], Wei Qin[a,b], Qian Guo[a,b], Jinbo Sun[a,b], Kai Yuan[a,b], Peng Liu[a,b], Yi Zhang[a,b], Karen M. von Deneen[d], Yijun Liu[d,e], Jie Tian[a,b,c,*]

[a] School of Electronic Engineering, Xidian University, Xi'an, Shaanxi 710071, China
[b] Life Sciences Research Center, School of Life Sciences and Technology, Xidian University, Xi'an, Shaanxi 710071, China
[c] Institute of Automation, Chinese Academy of Sciences, Beijing 100190, China
[d] Department of Psychiatry, McKnight Brain Institute, University of Florida, Gainesville, FL 32610, USA
[e] Department of Neuroscience, McKnight Brain Institute, University of Florida, Gainesville, FL 32610, USA

ARTICLE INFO

Article history:
Received 1 September 2009
Received in revised form 6 November 2009
Accepted 9 November 2009

Keywords:
Acupuncture
Time-varied
Graph theory analysis
Brain networks

ABSTRACT

Clinical acupuncture typically involves an effective treatment phase several hours post-therapy. We previously identified regions that carry the time-varied signals based on the BLOCK experimental paradigm. Here we characterize the brain network by applying the graph theory analysis during the post-acupuncture resting state. Our results show gradually increasing connections in the brainstem during verum acupuncture (ACU). The anterior insula plays an important role in connecting the components of the brain networks following ACU. We suggest that acupuncture can induce significant complex response patterns with relatively more robust magnitudes. Our findings provide direct evidence that the post-needling resting state contains acupuncture-related effects that are due to the slow-acting nature of acupuncture.

Introduction

Spontaneous fluctuations in blood oxygenation level dependent (BOLD) functional magnetic resonance imaging (fMRI) signals have recently aroused a large amount of interest in fMRI studies [9]. Functional connectivity analysis can investigate these coherent signal fluctuations, and reveal coactivation in a distributed network of cortical regions that characterizes the resting state of the human brain [11]. Evidence from acupuncture analgesia studies suggested that a delayed response exists during resting state following acupuncture stimulation [16].

Our group has compared different modulatory effects on resting brain networks between verum and sham acupuncture. Numerous studies indicated the existence of different functional brain networks [2,3,15,18,21,22]. Bai found that the activity pattern during the post-acupuncture rest epoch was prominently associated with stimulus-related effects by using the multi-GLM paradigm; some of the brain regions showed higher BOLD signal intensity during rest rather than in the stimulation phases [4]. Such time-varied characteristics of acupuncture effects attract more interest for their importance in designing paradigms and statistical models involving acupuncture studies. However, for limitations of GLM in modeling such state-related activity, a flexible model was needed to investigate the dynamics underlying sustained effects of acupuncture.

In our current study, we revealed the functional connectivity of acupuncture-evoked regions in terms of the correlation structure of their BOLD activity. Considering that acupuncture can be long-lasting even beyond the needling being performed, we examined the post-acupuncture resting state (PARS) and post-sham resting state (PSRS) functional connectivities using MRI. Graph theory analysis (GTA) was used to characterize the functional integrated network of time-varied activities induced by acupuncture. GTA has the advantages of evaluating the strength as well as the temporal and spatial patterns of interactions in the human brain [19], and it defines a graph as a set of nodes (brain regions) and edges (functional connections). The visualization of graph provides strong hints for functional connections between brain regions. Topological properties of the network could characterize prominent status and contribution to the continuous basis related to acupuncture. This approach has successfully been applied in many previous brain network studies with convincing results [1,14,20]. We experienced the challenges of functional connectivity development at an acupoint versus those at a non-meridian point (NMP) similar to the network analysis described in Fair's study [8]. In addition, the non-repeated event-related fMRI (NRER-fMRI) design was employed for investigating sustained effects after acupuncture administration. This new experimental paradigm was first used in Qin's research [18].

* Corresponding author at: Institute of Automation, Chinese Academy of Sciences, P.O. Box 2728, Beijing 100190, China. Tel.: +86 10 62527995; fax: +86 10 62527995.
E-mail address: tian@ieee.org (J. Tian).

0304-3940/$ – see front matter © 2009 Elsevier Ireland Ltd. All rights reserved.
doi:10.1016/j.neulet.2009.11.031

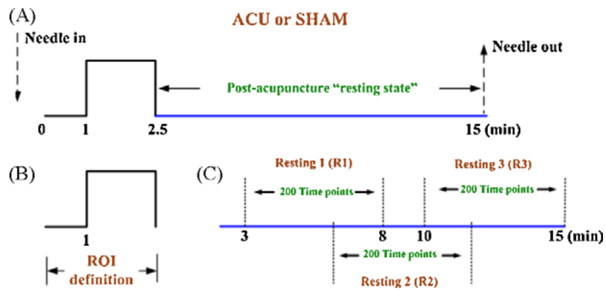

Fig. 1. Experimental paradigm. (A) The entire run lasted for 15 min. (B) Single BLOCK for ROIs definition. (C) PARS and PSRS for graph theory analysis.

Methods

All participants were recruited from a group of 28 right-handed college students (14 males and 14 females, 21.7 ± 1.9 (mean ± SD) years old). The subjects were acupuncture naïve and did not have a history of major medical illnesses, head trauma, neuropsychiatric disorders, had not used prescription medications within the last month, and had no contraindications for exposure to a high magnetic field. All subjects gave written, informed consent after the experimental procedures were fully explained, and all research procedures were approved by the West Chinese Hospital Subcommittee on Human Studies. The experiment was also conducted in accordance with the Declaration of Helsinki.

In the acupuncture experiment, all subjects were blinded to the type and order of stimulations. During the procedure, subjects were instructed to keep their eyes closed in order to prevent them from actually observing the procedures. The presentation sequence of the acupuncture and NMP protocols was randomized for all fMRI runs, and the order of presentation was counterbalanced across subjects. Acupuncture was performed at acupoint ST36 (Zusanli) on the right leg. The needles used in the acupuncture protocol were sterile disposable 38 gauge stainless steel acupuncture needle 0.2 mm in diameter and 40 mm in length. The needle was inserted perpendicularly to a depth of 2–3 cm. Stimulation consisted of rotating the needle clockwise and counterclockwise for 1 min at a rate of 60 times per min. The procedure was performed by the same experienced and licensed acupuncturist on all subjects. We employed the new NRER-fMRI design consisting of two functional runs: verum acupuncture (ACU) and sham acupuncture (SHAM). Only a single stimulation period was performed during each of these two runs (Fig. 1A). This NRER-fMRI design has the advantage of evaluating potential long-lasting effects following acupuncture administration. In ACU, an acupuncture needle was inserted at ST 36 for 1 min without manipulation and then the needle was manipulated for 1.5 min (Fig. 1B); the needle remained inserted in the acupoint for another 12.5 min. In SHAM, the procedure was the same as in ACU except that the stimula-

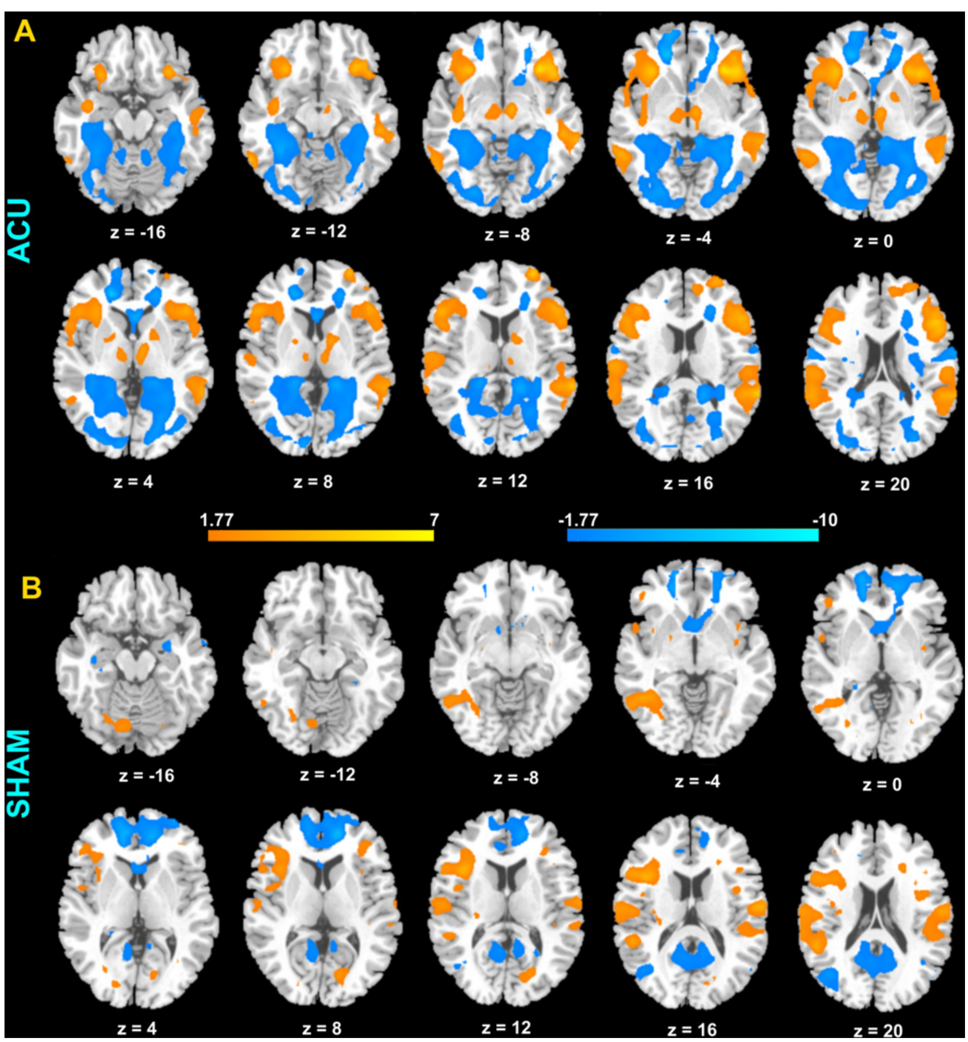

Fig. 2. Group results of brain activation for a single BLOCK.

tion was administered at a non-acupoint (2–3 cm apart from ST 36).

The experiments were carried out in a 3T GE scanner. A gradient echo T2*-weighted sequence with in-plane resolution of 3.75 mm × 3.75 mm (TE 30 ms, TR 2 s, matrix 64 × 64, FOV 240 mm, flip angle 90°) and a set of T1-weighted high-resolution structural images were acquired (TE 3.39 ms, TR 2.7 s, matrix 256 × 256, FOV 256 mm, flip angle 7°, in-plane resolution 1 mm × 1 mm, slice thickness 1 mm).

The first 100 time points (single BLOCK) including the acupuncture stimulus were recruited to localize regions of interest (ROIs) for further analysis (Fig. 1B). Data preprocessing steps included: rigid body correction for geometrical displacements caused by head movement; co-registration with the Montreal Neurological Institute (MNI) EPI template image; and image smoothing with a 6 mm Gaussian kernel to decrease spatial noise. Standard general linear model (GLM) was then calculated. For the comprehensive evaluation of the PARS and PSRS networks in the GTA, a conservative threshold of $p < 0.05$ (uncorrected) was chosen. ROIs were derived from the union of activated brain regions by creating 6-mm diameter spheres around the activated center of mass coordinates in ACU and SHAM.

To characterize the inter-regional relations for our defined ROIs, GTA defined a graph as a set of nodes and edges [6]. Both

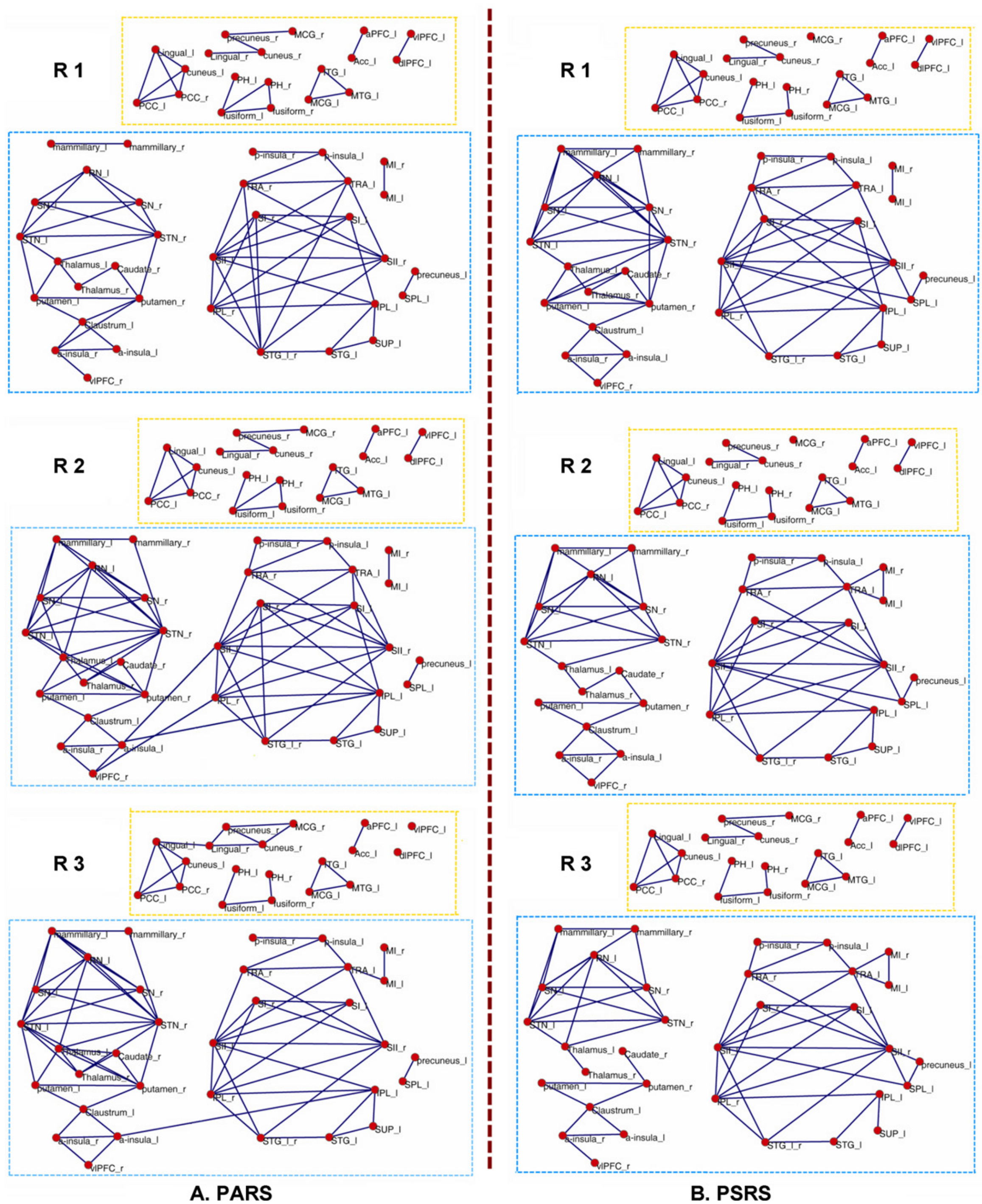

Fig. 3. Graph formed from (A) PARS and (B) PSRS.

Table 1
ROIs sorted into components based on the group results of single BLOCK.

Regions of interest (ROIs)			Talairach		
			x	y	z
Ventrolateral prefrontal cortex	(vlPFC)	L	−30	20	−4
		R	45	26	−9
Anterior prefrontal cortex	(aPFC)	L	−15	49	−5
		R	30	59	5
Dorsolateral prefrontal cortex	(dlPFC)	L	−53	27	10
		R	9	51	28
Orbito frontal cortex	(OFC)	L	−24	43	−7
		R	24	43	−10
Anterior cingulate cortex	(Acc)	L	−12	46	−5
Somatosensory cortex	(SI)	L	−59	−19	26
		R	65	−19	29
Parahippocample	(PH)	L	−30	−35	−6
		R	36	−44	−5
Posterior cingulate cortex	(PCC)	L	−9	−64	11
		R	12	−52	8
Middle occipital cortex	(MCG)	L	−53	−59	−5
		R	15	30	26
Middle cingulate cortex	(MCC)	L	−15	−18	40
		R	9	25	32
Inferior paretal lobule	(IPL)	L	−59	−39	27
		R	62	−22	29
Secondary somatosensory cortex	(SII)	L	−62	−22	18
		R	56	−23	15
Primary motor cortex	(MI)	L	−62	−8	22
		R	65	−5	20
Superior paretal lobule	(SPL)	L	−18	−47	60
		R	27	−62	50
Superior temporal gyrus	(STG)	L	−53	−40	21
		R	65	−34	18
Middle temporal gyrus	(MTG)	L	−53	−58	−2
		R	59	−1	−15
Supramarginal	(SUP)	L	−56	−39	30
Inferior temporal gyrus	(ITG)	L	−56	−61	−4
		R	45	−67	1
Transverse temporal	(TRA)	L	−56	−14	12
		R	65	−17	12
Anterior insula	(a-insula)	L	−39	20	2
		R	36	20	3
Posterior insula	(p-insula)	L	−43	−15	−2
		R	42	−14	−5
Substania nigra	(SN)	L	−6	−12	−9
		R	9	−15	−7
Subthalamic nucleus	(STN)	L	−12	−15	−4
		R	9	−12	−4
Red nucleus	(RN)	L	−6	−18	−2
Cuneus		L	−9	−58	6
		R	18	−81	10
Lingual		L	−9	−59	3
		R	27	−67	1
Claustrum		L	−33	9	0
Caudate		L	−6	−17	−1
		R	6	17	−1
Fusiform		L	−30	−33	−16
		R	30	−41	−11
Pons		R	0	−39	−28
Putamen		L	−18	3	0
		R	18	3	0

Table 1 (*Continued*)

Regions of interest (ROIs)		Talairach		
		x	y	z
Mammillary	L	−3	−12	−7
	R	3	−12	−7
Thalamus	L	−9	−27	7
	R	6	−14	9
Precuneus	L	−18	−50	55
	R	27	−75	20

PARS and PSRS were divided into three parts for evaluating the development of the brain network (Fig. 1C). In our study, we applied the correlation method described in Salvador to construct our network [20]. Preprocessing for GTA was carried out exactly as described in Salvador's research [20]. The preprocessing steps and the statistical analysis were all performed with SPM5 software.

Results

Group results for acupuncture at ST36 showed extensive signal changes in the limbic/paralimbic areas, neocortical regions, brainstem and cerebellum (Fig. 2). These brain activations were also found in our previous study [4]. Sixty-three putative acupuncture-evoked ROIs were derived from the group results in the single BLOCK. From three parts of PARS and PSRS (Fig. 1C), the time course of each ROI was correlated to every other ROI to obtain a 63×63 matrix of correlation coefficients, and the mean functional connectivity matrix was computed by averaging the entire correlation matrix. We then created an unweighted binary graph so that the nodes were connected if the correlation coefficients exceeded the threshold (Fisher's r-to-z transformation was applied). For directly analysis the brain network, single nodes were deleted by the artificial settings.

As shown in Fig. 3, the PARS and PSRS networks were separated into two main parts. The larger component consisted of 33 ROIs in the brainstem, striatum and sensorimotor cortex. The anterior insula and IPL also belong to this component. The characteristic of this component changed over time. The remaining component consisted of the fusiform, midoccipital cortex and lingual regions and parts of the brain default model network [10]. This component presented the steady structure in the three parts of the resting state.

Discussion

After searching PubMed, our group was the first to provide evidence to support the idea that acupuncture is a slow-acting agent and has a specific pattern of the dynamic for the entire coupled nervous system [4]. The current study was a preliminary investigation on the sustained effects of acupuncture during the resting state. GTA was applied to describe the functional connectivity patterns among the defined ROIs (Table 1). Based on the different structures of connectivity patterns of the network (Fig. 3A), we proposed that the development of brain networks over time reflected the long-lasting effect following acupuncture.

Several acupuncture studies have already emphasized the important neural activity of the midbrain nuclei on the endogenous monoaminergic and opioidergic systems [3,12,13]. From our results using GTA, the ROIs located in the brainstem were strongly connected with each other following acupuncture at both ST36 and NMP during R1, which was consistent with our previous study showing that brain activity in the brainstem during rest was prominently associated with acupuncture-related effects [3,4].

However, by comparing the topological properties of the networks in ACU and SHAM, the functional connectivity patterns developed in distinct ways during three sequential periods of the resting state. During R2, the brain network following ACU had more complex links between the brainstem structures, striatum, thalamous and anterior insula (a-insula). Such complicated functional connection patterns were also maintained during R3 (Fig. 3A). On the other hand, the SHAM network exhibited contrary results with relatively sparse links found during R2 and R3 (Fig. 3B). These results were consistent with Bai's research that ACU could induce significant complex response patterns and relatively more robust magnitudes [4]. The gradually increasing involvement of the brainstem suggested that acupuncture could induce large distributions of time-varied BOLD responses. It may also suggest that the brainstem plays a critical role in the descending antinociceptive pathway of the central nervous system mechanism of acupuncture [3]. We found further support that the different network structure may stem from resource redistribution due to the different function-guide actions between ACU and SHAM [15].

An intriguing finding was the close relationship between the a-insula and sub-networks. The a-insula was identified as the bridge that connected the components of the brain networks following ACU (Fig. 3A), whereas this was not found in SHAM (Fig. 3B). It seemed conclusive that the a-insula exhibited centrality in ACU. Several studies proposed the importance of the a-insula, suggesting that it may have a core role for task set implementation [5,7]. Mesulam and Mufson also pointed out that abundant connections and a functional interface between the limbic system and the neocortex make the insula as a unique position to assign significance to the sensory information it receives [17]. Given that acupuncture mediates the neurophysiological system with more voluntary components of self-control and self-regulation to restore homoeostasis, we inferred that the insula may engage in monitoring the ongoing modulation of acupuncture effects on the internal states of the organism.

Another component of the network consisting of 19 ROIs is primarily located in the occipital cortices and parts of the brain's default model network. This sub-network remained stable over time (Fig. 3). Due to the same somatosensory manipulation performed on both ACU and SHAM during resting state, it was not surprising to see the steady involvement of the sub-network connection in our results. These findings suggested that low-frequency oscillations and correlations may reflect endogenously coordinated changes in the entire neural system.

Limitation

The application of GTA to the PARS and PSRS fMRI data is a nascent field of research. As a result, our analyses for the development of distinct brain networks were limited to a set of 63 predefined ROIs. Therefore, we may not have described comprehensive characteristic of acupuncture network. Further evidence need to be investigated in the brain functional network after acupuncture manipulation.

Conclusion

Our results have provided direct evidence that the post-needling resting state contained acupuncture-related effects because of the slow-acting agent of acupuncture. Complex systems in acupuncture seem to be affected by different components in the brain networks that can be found by operating at different time periods. These sustained effects may reflect a significant characteristic underlying acupuncture.

Acknowledgements

We thank Dr. Qiyong Gong and the research staff at the West China Hospital for their assistances in carrying out the experiment and data collections. This paper is supported by Changjiang Scholars and Innovative Research Team in University (PCSIRT) under Grant No. IRT0645, the Chair Professors of Cheung Kong Scholars Program of Ministry of Education of China, CAS Hundred Talents Program, the Joint Research Fund for Overseas Chinese Young Scholars under Grant No. 30528027, the National Natural Science Foundation of China under Grant Nos. 30970774, 60901064, 30873462, 90209008, 30870685, 30672690, 30600151, 60532050, 60621001, the Beijing Natural Science Fund under Grant No. 4071003, the Knowledge Innovation Program of the Chinese Academy of Sciences under Grant No. KGCX2-YW-129, the Project for the National Key Basic Research and Development Program (973) under Grant No. 2006CB705700, and 863 program under Grant No. 2008AA01Z411.

References

[1] S. Achard, R. Salvador, B. Whitcher, J. Suckling, E. Bullmore, A resilient, low-frequency, small-world human brain functional network with highly connected association cortical hubs, Journal of Neuroscience 26 (2006) 63–72.
[2] L.J. Bai, W. Qin, J. Tian, J. Dai, W. Yang, Detection of dynamic brain networks modulated by acupuncture using a graph theory model, Progress in Natural Science, in press.
[3] L.J. Bai, W. Qin, J. Tian, M.H. Dong, X. Pan, P. Chen, J. Dai, W. Yang, Y.J. Liu, Acupuncture modulates spontaneous activities in the anticorrelated resting brain networks, Brain Research (2009) 37–49.
[4] L.J. Bai, W. Qin, J. Tian, P. Liu, L.L. Li, P. Chen, J.P. Dai, J.G. Graggs, K.M. Deneen, Y.J. Liu, Time-varied characteristics of acupuncture effects in fMRI studies, Hunam Brain Mapping (2009) 3445–3460.
[5] T.S. Braver, D.M. Barch, Extracting core components of cognitive control, Trends in Cognitive Sciences 10 (2006) 529–532.
[6] N.U.F. Dosenbach, D.A. Fair, F.M. Miezin, A.L. Cohen, K.K. Wenger, R.A.T. Dosenbach, M.D. Fox, A.Z. Snyder, J.L. Vincent, M.E. Raichle, Distinct brain networks for adaptive and stable task control in humans, Proceedings of the National Academy of Sciences 104 (2007) 11073–11078.
[7] N.U.F. Dosenbach, K.M. Visscher, E.D. Palmer, F.M. Miezin, K.K. Wenger, H.C. Kang, E.D. Burgund, A.L. Grimes, B.L. Schlaggar, S.E. Petersen, A core system for the implementation of task sets, Neuron 50 (2006) 799–812.
[8] D.A. Fair, N.U.F. Dosenbach, J.A. Church, A.L. Cohen, S. Brahmbhatt, F.M. Miezin, D.M. Barch, M.E. Raichle, S.E. Petersen, B.L. Schlaggar, Development of distinct control networks through segregation and integration, Proceedings of the National Academy of Sciences 104 (2007) 13507–13512.
[9] M.D. Fox, M.E. Raichle, Spontaneous fluctuations in brain activity observed with functional magnetic resonance imaging, Nature Reviews Neuroscience 8 (2007) 700–711.
[10] M.D. Fox, A.Z. Snyder, J.L. Vincent, M. Corbetta, D.C. Van Essen, M.E. Raichle, The human brain is intrinsically organized into dynamic, anticorrelated functional networks, Proceedings of the National Academy of Sciences 102 (2005) 9673–9678.
[11] M.D Greicius, G. Srivastava, A.L. Reiss, V. Menon, Default-mode network activity distinguishes Alzheimer's disease from healthy aging: evidence from functional MRI, Proceedings of the National Academy of Sciences 101 (2004) 4637–4642.
[12] S.H. Han, S.H. Yoon, Y.W. Cho, C.J. Kim, B.I. Min, Inhibitory effects of electroacupuncture on stress responses evoked by tooth-pulp stimulation in rats, Physiology & Behavior 66 (1999) 217–222.
[13] K.K.S. Hui, J. Liu, O. Marina, V. Napadow, C. Haselgrove, K.K. Kwong, D.N. Kennedy, N. Makris, The integrated response of the human cerebro-cerebellar and limbic systems to acupuncture stimulation at ST 36 as evidenced by fMRI, Neuroimage 27 (2005) 479–496.
[14] J.X. Liu, J.M. Liang, W. Qin, J. Tian, K. Yuan, L.J. Bai, Y. Zhang, W. Wang, Y.R. Wang, Q. Li, L. Lu, K. Deneen, Y.J. Liu, M. Gold, Dysfunctional connectivity patterns in chronic heroin users: an fMRI study, Neuroscience Letters (2009) 72–77.
[15] P. Liu, W. Qin, Y. Zhang, J. Tian, L. Bai, G.Y. Zhou, J.X. Liu, P. Chen, J. Dai, Combining spatial and temporal information to explore function-guide action of acupuncture using fMRI, Journal of Magnetic Resonance Imaging, in press.
[16] D.J. Mayer, Biological mechanisms of acupuncture, Progress in Brain Research 122 (2000) 457–477.
[17] M.M. Mesulam, E.J. Mufson, Insula of the old world monkey. III. Efferent cortical output and comments on function, The Journal of Comparative Neurology 212 (1982) 38–52.
[18] W. Qin, J. Tian, L.J. Bai, X.H. Pan, Y. Lin, P. Chen, J.P. Dai, A. Lin, B.X. Zhao, Q.Y. Gong, W. Wang, K.M. Deneen, Y.J. Liu, FMRI connectivity analysis of acupuncture effects on an amygdala-associated brain network, Molecular Pain 4 (2008) 55.
[19] J.C. Reijneveld, S.C. Ponten, H.W. Berendse, C.J. Stam, The application of graph theoretical analysis to complex networks in the brain, Clinical Neurophysiology 118 (2007) 2317–2331.

[20] R. Salvador, J. Suckling, M.R. Coleman, J.D. Pickard, D. Menon, E. Bullmore, Neurophysiological architecture of functional magnetic resonance images of human brain, Cerebral Cortex 15 (2005) 1332–1342.
[21] Y. Zhang, J. Liang, W. Qin, P. Liu, K. Deneen, P. Chen, L.J. Bai, J. Tian, Y.J. Liu, Comparison of visual cortical activations included by electro-acupuncture at vision and nonvision-related acupoints, Neuroscience Letters (2009) 6–10.
[22] Y. Zhang, W. Qin, P. Liu, J. Tian, J.M. Liang, K.M. Deneen, Y.J. Liu, An fMRI study of acupuncture using independent component analysis, Neuroscience Letters 449 (2008) 6–9.